

USING EISCAT RADARS FOR SPACE DEBRIS DETECTION

Markku S. Lehtinen¹, Jussi Markkanen², Antero Väänänen³, and Asko Huuskonen⁴

¹ University of Oulu, Sodankylä, Finland, Email: markku.lehtinen@sgo.fi

² University of Oulu, Sodankylä, Finland, Email: jussi.markkanen@sgo.fi

³ Sodankylä Geophysical Observatory, University of Oulu, Sodankylä, Finland, Email: antero.vaananen@sgo.fi

⁴ Finnish Meteorological Institute, Helsinki, Finland, Email: asko.huuskonen@fmi.fi

ABSTRACT

As ESA contract work, we are studying the feasibility of using the EISCAT incoherent scatter radars for space debris measurements. Tests at two EISCAT sites demonstrate that this indeed is possible, and can proceed in parallel with normal EISCAT ionospheric work, using a separate receiver back end to record the raw sample stream. Early analysis of the data suggests that, after coherent integration of the signal, particles of size 3 cm in the center of the antenna beam are detectable from 1000 km range.

1. INTRODUCTION

The EISCAT incoherent scatter radar system in Northern Scandinavia and on Svalbard is one of the most sophisticated of its kind worldwide. The system consists of three separate radars: monostatic VHF radar, located near Tromsø, Norway and operating at 224 MHz, monostatic but two-antenna EISCAT Svalbard Radar in Longyearbyen, Svalbard, operating at 500 MHz, and tristatic EISCAT UHF radar at 929 MHz, with transmitter/receiver in Tromsø and receivers also in Kiruna, Sweden, and Sodankylä, Finland. All the transmitters operate in the MW peak power range and have duty cycles between ten and twenty percents. However, until now the EISCAT radars have not been used for measuring hard targets.

As contract work between ESA/ESOC and Sodankylä Geophysical Observatory (SGO), we have started in February 2000 a feasibility study of using the EISCAT radars for detection of small size space debris (SD). The goal is to be able to conduct SD measurements in parallel with normal EISCAT ionospheric work. A large portion of the 2000 hours that EISCAT normally measures annually, could then also be utilized for SD measurements.

on the UHF system. We perform a simple sensitivity comparison between the EISCAT radars. Then we describe the special workstation based receiver that we have used to measure in parallel with the EISCAT receivers, and sketch the signal processing involved. Next, we summarize our detection/parameter estimation framework which we express in terms of statistical inversion theory. We show a few detection examples from our measuring campaigns at EISCAT. We finish by stating our preliminary conclusion.

2. THE EISCAT RADARS

2.1. The UHF System

An overall block diagram of the Tromsø UHF system is shown in Fig. 1. The UHF transmitter consist of the following main subunits

- ▷ A frequency generating module, the exciter
- ▷ An intermediate power amplifier.
- ▷ Two klystron power amplifiers, each rated to 1.3 MW. At the moment, problems in the waveguide system limit the maximum combined output power to about 1.5 MW.
- ▷ Modulation system for pulses and binary phase codes.

The maximum transmission duty cycle is rated to 12.5%, typical values being 8%–10%. Before antenna feed horn, there is a polarizer unit that is used to give circular polarization to the outgoing wave (other polarizations are possible but not used in practice).

On the receiver side, after the polarizer, the UHF system has a receiver protector, followed by a preamplifier. The preamplifier is cooled to the physical temperature about 30 K, but the need of the protector, together with sky noise, causes the actual system noise temperature to be around 80 K.

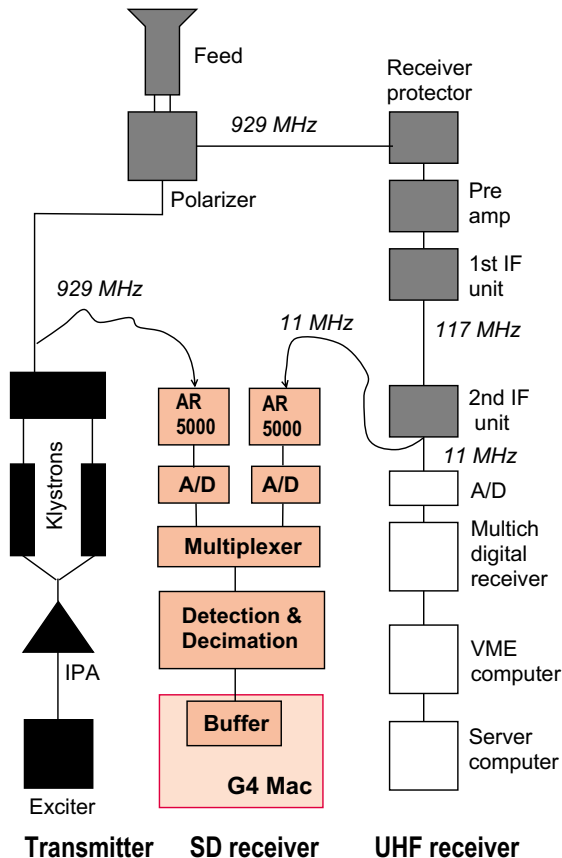


Figure 1. EISCAT UHF radar and our SD receiver

around 117 MHz. The IF1 is taken down from the antenna to the receiver hall where it is downconverted to the second intermediate frequency (IF2) about 11 MHz. The analog signal path is bandlimited to 7 MHz by a filter centered at 11.25 MHz.

The second IF is digitized by a 14-bit A/D converter, which produces a continuous sample stream at a rate of 15 Msamples/s. This stream is fed to a digital multichannel receiver backend, for subsequent detection, decimation, filtering and postprocessing. In normal EISCAT experiments, various autocorrelation estimates are formed by the processing computers and recorded to disk.

The UHF antenna is a parabolic mirror of 32 m diameter with Cassegrain optics. The antenna is fully steerable both in azimuth and in elevation.

2.2. Other EISCAT Radars

At the Tromsø site there is located also the EISCAT VHF radar. This has a large cylindrical-parabolic antenna of dimension 120 m × 40 m. The antenna is steerable only in elevation. The VHF transmitter and receiver are basically similar to the UHF system.

The newest site to the EISCAT family, the EISCAT

number seven, on a mountainside ten kilometers from Longyearbyen, Svalbard, at latitude 78° North. The ESR transmitter has sixteen standard Thomson TV klystrons, with combined peak power 1.0 MW and the high duty cycle of 25%. The transmitter can be switched, from pulse to pulse if required, between the two ESR antennas: a 32 m fully steerable antenna and a 42 m antenna with fixed pointing. There are two separate receivers, both quite similar to the Tromsø receivers, with cooled preamplifier and digital backend.

2.3. Sensitivity Comparison

The backscatter cross section of a conducting sphere of diameter d can be approximated by the Rayleigh formula $9\pi^4 \left(\frac{d}{\lambda}\right)^4 \sigma_0$, where σ_0 is the geometrical cross section and λ the radar wavelength. This approximation is good for d/λ less than about 0.2. For larger diameter, the cross section first oscillates and then converges towards the geometrical cross section.

The Rayleigh formula, together with the standard radar equation involving antenna gain, wavelength and the target distance, allows one to estimate the received backscatter power on the beam optical axis.

Small sized, slowly moving targets tend to produce highly coherent echoes. This characteristic property can be used to improve the odds of detection in a noisy environment, by ensuring that the signal samples are added with fixed phase. This is called coherent integration. In this case, the signal variance goes down proportionally to the integration time.

If the incoming sinusoidal signal has amplitude A and is integrated coherently over N samples, the effective signal to noise after the integration is

$$\text{SNR}_N \equiv \frac{|A|^2}{\sigma^2/N}$$

where σ is the root mean square value of the noise.

The amount of integration is determined by the signal duration. For instance, in a 0.1 s measurement with 20 % transmission duty cycle and one microsecond sampling interval, one gets $N = 20000$ signal samples.

To compare the detection sensitivity of several radars, with different wavelengths, antenna gains, peak powers, system temperatures and maximum duty cycles, in a way that gives some feeling about the detectable size, we have computed into Table 1 a “reference diameter” d_{ref} . This we define as the diameter of the sphere which gives $\text{SNR}_N = 1$ from 1000 km range, with 0.1 s data collection interval. The ESR system in Table 1 is the 42 m antenna.

Table 1 indicates that when hunting small targets, the UHF is the most sensitive of the EISCAT radars.

Table 1. Sensitivity comparison

	VHF	ESR	UHF	fgan
Antenna gain (dB)	43.1	45.3	48.1	49.7
Wavelength (cm)	134	60	32	22
Peak power (MW)	3.0	1.0	2.0	1.6
Max duty cycle (%)	12.5	25.0	12.5	3.7
Noise temp. (K)	300	60	80	209
d_{ref} (cm)	3.4	1.8	1.2	1.4

In practical circumstances the actual detection limit can be expected to be considerably larger than d_{ref} . For one thing, one normally needs to search for the target over large set of ranges, and in this case the condition $\text{SNR}_N = 1$ is quite too weak to ensure reliable detection. Radar signals also often contain disturbances and distortions which will confuse the detection. The signal and/or the radar system itself might not be as coherent as we are assuming either. Finally, most targets will not pass through the beam center, and so the actual number of detectable events will depend also on the antenna beam shape.

3. SPACE DEBRIS RECEIVER

To be able to measure in parallel with EISCAT, an additional data collecting system is needed. Coherent integration requires that the raw samples are available. The present EISCAT receiver does not offer such a data stream as a service to anybody (including itself). We have used a separate receiver of our own for the data collection, hooking it to the EISCAT system at the second IF level.

In this section we describe our SD receiver, as used in recent campaign on Tromsø UHF, February 2001. Fig. 1 shows the main blocks of the SD receiver and its connections to the EISCAT receiver.

Noting the EISCAT transmission flexibility, we are not counting in knowing the transmission a priori. Instead, we sample fast enough to always cover the whole relevant IF2 band. The widest band needed during the February campaign was 2.1 MHz. It was sampled at 2.5 Msamples/s (complex). The individual EISCAT frequency channels are rather narrow-band, a few hundred kHz at most, so the IF band has large gaps without any useful information. We plan to later compress our data, by cutting off the empty segments. Preferably this should happen already on-line.

In addition to the normal reception channel, we also need sample during the transmission periods, to get the code patterns. At its ESR site, EISCAT provides the transmission samples on the same data path than the reception, so no special arrangements are needed there. In Tromsø, this service is planned but not yet

Our data acquisition system has originally been developed for ionospheric tomography by a company called Invers Oy. The basic system consists of a sampling section, a detection/decimation section and an output section.

In this case, the raw sampling rate was 40 MHz. This 25 ns stream is processed by programmable logic to perform detection, essentially by doing a Hilbert transform (quarter wavelength sampling). The output samples are rearranged to correspond to a 10 MHz complex sample stream, or a suitably decimated version thereof, and written into the output buffer. The decimation is done by adding an appropriate number of consecutive complex samples, thus ensuring proper filtering.

It may be noted that no separate conversion to baseband is done in this system. What one has in the baseband is some Nyquist replica of the positive frequency part (or the negative frequency part) of the original, real-valued analog signal. To work, this arrangement requires the bandlimited analog input to be centered on a suitable frequency. The necessary frequency translation is done by a commercial radio, here the AR5000 broadband communication receiver, placed in front of the analog to digital converter.

The output buffer is mounted on a PCI slot of a fast workstation. We are using Power Mac G4 workstations, running under the Mac OS X version of UNIX. Software from the Invers Oy is used to read the data and write it to hard disks. Typical data accumulation rate is between 20-30 Gbytes/hour, depending on the sampling interval. For final storage, data is copied to Firewire disks.

In addition to the samples, 1 second time tick from EISCAT GPS and a transmission on/off flag were included into the recorded data stream.

All subsequent data processing has been done off-line.

4. DETECTION AND PARAMETER ESTIMATION

Assuming constant radial acceleration, target distance r from the radar during a single integration can be written as

$$r(t) = R + v_r t + \frac{1}{2} a_r t^2$$

with R , v_r and a_r constants. The received, detected complex signal is then modelled as a Doppler-shifted replica of the transmission ϵ^T

$$s(t) = A \cdot \epsilon^T \left(t - \frac{2r}{c} \right) \cdot e^{i\omega_D t} \cdot e^{i\alpha_D t^2}$$

$\omega_D = \frac{2\omega_{RF}}{c} \cdot v_r$ is Doppler frequency
 $\alpha_D = \frac{\omega_{RF}^2}{c} \cdot a_r$ is "Doppler acceleration"
 ω_{RF} is transmission frequency

We base target detection on comparison of the signal strength against a suitably chosen threshold level

$$\text{detection} \Leftrightarrow |\hat{A}| > \text{Threshold}$$

Therefore, we need an estimate of the signal amplitude A . In addition to the amplitude, we want estimates for R , ω_D and α_D as well.

A suitable tool to compute these estimates is the quantity that sometimes is called the radar ambiguity function. Here we will — hopefully more descriptively and less ambiguously — instead use the term generalized match function, GMF. For sampled signals, the GMF is defined by

$$\text{GMF}(\omega, R, \alpha) \equiv \frac{|\langle s + n, \epsilon^T(t - \frac{2R}{c})e^{i\omega t}e^{i\alpha t^2} \rangle|}{\langle \epsilon^T, \epsilon^T \rangle} \quad (1)$$

The notation $\langle \cdot, \cdot \rangle$ means the standard inner product of complex vectors, and $n(t)$ is the noise process. Using the GMF, the parameter estimation reduces to finding the GMF maximum point:

- ▷ The position of the GMF maximum gives the estimates \hat{R} , $\hat{\omega}$, $\hat{\alpha}$.
- ▷ The value of the GMF maximum gives $|\hat{A}|$.

This result can be derived in various ways, of which we prefer the viewpoint of (Bayesian) statistical inversion. In that framework, the estimate represents the maximum point of the a posteriori probability density. Statistical inversion gives a well defined way to feed a priori probability information into the detection problem. We have not made actual use of this option so far, but it is not inconceivable to do so later, when we have better ideas about the parameters of the SD population.

We note that the above GMF maximum point also corresponds to the maximum likelihood estimate of the signal parameters.

For a given range gate R_j and acceleration α_m , the GMF can be computed over full set of frequencies by a single FFT. To find the maximum, the function must be evaluated over a tight 3D grid. Even with the FFT, this is very tedious, and so far we have ignored the acceleration.

In our scanning programs, we normalize the GMF by expressing the observed signal $s + n$ in terms of the r.m.s of the integrated noise, σ/\sqrt{N} . We perform the detection in two phases. We first compute

$$\text{Ratio}(r) \equiv \max_{\omega} \text{GMF}(\omega, r) / \frac{\sigma}{\sqrt{N}} \quad (2)$$

and then compare maximum of the *Ratio* against a threshold. This two-phase scheme gives useful visual

5. DETECTION EXAMPLES

5.1. ESR Data

In Nov 1999, before we had entered the present contract, we conducted an experiment campaign at the ESR site, using an earlier version of the SD receiver. The EISCAT experiment running at that time was the "tau0" experiment, which is the most popular experiment at ESR. The experiment transmits in two frequencies. The modulation pattern contains a set of phase codes, with baud length $60 \mu\text{s}$. The experiment has 20% duty cycle. The 42 m antenna was used, so pointing was fixed to azimuth 181.6° , elevation 81.6° . We took data at the rate of 0.5 Msamples/s (complex) with our own receiver.

We have done a SD search through our longest contiguous data set, 45 min. The search parameters were the following

- time step: 1.0 s
- integration: 100 ms
- range interval: 390-1130 km,
- range step: 3.0 km
- threshold: 5.0

Our software found 32 events, of which at least 26 appear to be different, genuine targets. The latter conclusion is based on various high time resolution rescans of the data, where we have inspected time series of the target parameters. All the unambiguous events were on ranges larger than 650 km, and had radial velocities less than 1.4 km s^{-1} .

For all detected events, our scanning software also computes the "equivalent diameter", which we define to be the diameter of a sphere which, from the measured range but otherwise under the assumptions of Table 1, would produce the observed amplitude.

Unfortunately, in almost all cases, *none* of the required assumptions will be valid. The estimate can be wrong per se, the system temperature might have changed, the transmission power might not have been maximal. The most serious uncertainty is that the particle might not have been anywhere near the center of the antenna beam.

It would be possible to get both the transmission power and the actual system temperature from the data and the EISCAT parameters, and with sufficiently high threshold value, the amplitude estimate for an accepted event should be reliable. But finding the actual position of the target with respect to the beam center is a major unsolved problem in this project. Thus the equivalent diameter must be viewed with suspicion. Nevertheless, it was computed, and was between 2.4 cm and 18 cm in the original detection scans.

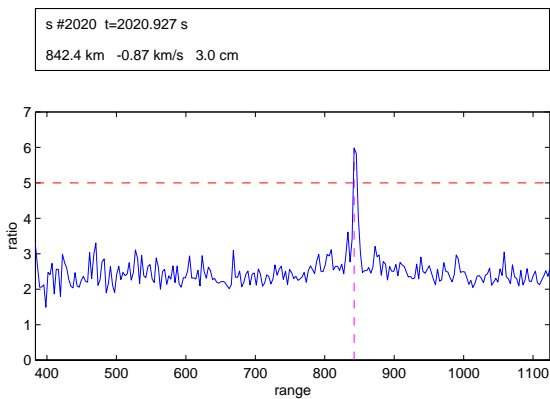


Figure 2. SD detection, ESR data

quantity Ratio, defined in Eq. 2. The normalized detection threshold 5.0 is indicated by the horizontal dashed line. The vertical dashed line shows the location of the the maximum of Ratio(r). This value is used as the range estimate. The equivalent diameter was 3.0 cm.

However, when re-scanning the data with smaller time steps around this event, higher amplitude value (23.3) was found, corresponding to equivalent diameter of 4.7 cm. It is possible that this target did not cross the main beam at all, in which case its physical size must have been more than 15 cm.

5.2. UHF Data

Our longest contiguous data set from Feb 2001 on Tromsø UHF is about three hours of the “cp11t” experiment, which is the most popular experiment on this radar. We have done a coarse scan on the data, though only on the range interval 300–600 km that happens to be most easily accessible to analysis.

It is known that the number of SD particles decreases when going to lower altitudes, but even then, after the crowded sky of Svalbard, we are a little puzzled to find only a single clear event now. The target was found at range 506 km (altitude 493 km), and had equivalent diameter 2.7 cm.

High time resolution scan around this event is shown in Fig. 3. The top curve shows the estimated signal power (arbitrary units). The symmetric shape suggest that the particle traversed (somewhere) through the main beam in this case. The middle curve gives the range, and the bottom curve the Doppler velocity.

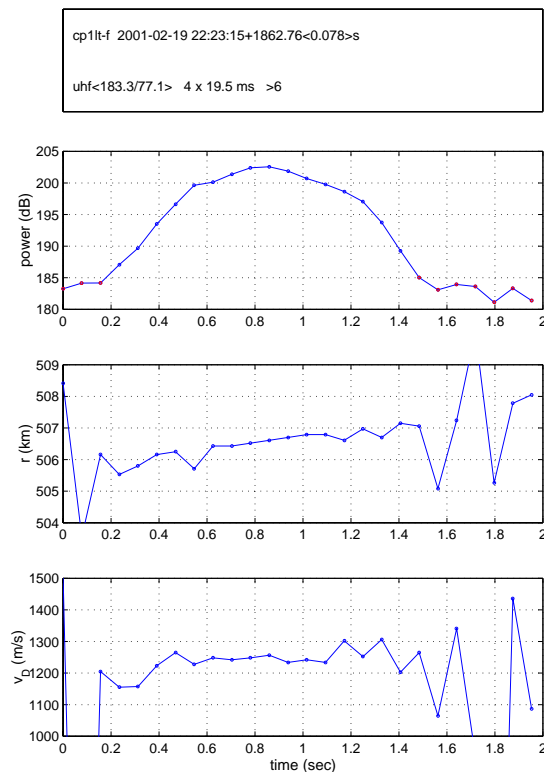


Figure 3. SD event in Tromsø UHF

6. SUMMARY

EISCAT radars can be used for parasitic SD detection. Our measurements at the ESR and Tromsø UHF show that there is no practical problem in capturing EISCAT analog signal, sampling it fast enough to cover the frequency band used by standard EISCAT experiments, and write the samples to disk. Doing this does not harm the normal EISCAT operation.

Both the ESR and the UHF radars are sensitive enough to measure particles of few centimeters in diameter. At ESR, a 45 minutes run found more than 20 clear targets at altitudes 650–1100 km, with equivalent diameters down to about 3 cm.

The main problem is the high data accumulation rate, on the order of 20 GBytes/hour. To achieve real time detection requires both faster detection computations – which we are in the process of implementing – and more raw computing power.